Polymer Chemistry

ROYAL SOCIETY OF CHEMISTRY

PAPER

View Article Online
View Journal | View Issue

Cite this: *Polym. Chem.*, 2024, **15**, 4454

Acid-labile and non-degradable cross-linked star polymer model networks by aqueous polymerization for *in situ* encapsulation and release†

Gavin Irvine, [a] Stuart Herron,[a] Daniel W. Lester [b] and Efrosyni Themistou *[a]

Received 12th June 2023,
Accepted 11th October 2024

DOI: 10.1039/d3py00677h

rsc.li/polymers

Biocompatible, acid-labile cross-linked star polymer model networks (CSPMNs) have great potential for use in drug delivery. However, a primary complication of this research stems from the prevalence of their synthesis to take place in organic solvents. Herein, to minimize CSPMN potential cytotoxicity, aqueous reversible addition–fragmentation chain transfer polymerization is employed for their synthesis. Initially, "arm-first" star polymers were synthesized in water using a poly[oligo(ethylene glycol) methyl ether methacrylate] (POEGMA) homopolymer and a non-degradable ethylene glycol dimethacrylate or acid-labile diacetal-based bis[(2-methacryloyloxy)ethoxymethyl] ether cross-linker. Subsequently, OEGMA addition resulted in the preparation of "in–out" star polymers (with higher molecular weights) followed by cross-linker addition to form CSPMNs. Rhodamine B dye encapsulation was performed during CSPMN synthesis and its release was observed under biologically relevant conditions. Having shown the effective breakdown of the diacetal-based CSPMNs, their potential for use in drug delivery in low pH environments (*i.e.* cancerous tumors) is expected to be high.

Introduction

Biocompatible synthetic polymer hydrogels[1] (water-swellable polymer networks) are attracting increasing attention as drug delivery systems, tissue engineering matrices and biosensors, due to their ability to absorb large quantities of water or biological fluids.[2] A class of these materials, with great structural control, is polymer model networks,[3] prepared by "living" polymerization techniques.[4] These polymer networks have well-defined structures consisting of precise lengths of (elastic) chains between their cross-links and therefore, it is expected that they can give more consistent and predictable results when used multiple times in a specific application.

A relatively new type of model network developed by Patrickios and coworkers in 2001[5] is that of CSPMNs[6] comprising interconnected "in–out" star polymers. These model networks are based on cross-linked star polymers bearing both elastic and dangling chains and two different types of cores, the primary and the secondary. The primary cores have both elastic and dangling chains connected to them, whereas the secondary cores bear only elastic chains. Various types of CSPMNs, such as homopolymer hydrophilic,[5] amphiphilic,[7–10] double-hydrophilic,[11,12] acid-labile[13–15] and double network amphiphilic,[16–20] were synthesized by the Patrickios group using various monomers and two different polymerization techniques, group transfer polymerization (GTP)[21,22] at ambient temperature[5,8–16,23] and reversible addition–fragmentation chain transfer (RAFT) polymerization[24,25] at 65[19]–70 °C.[18] However, the research surrounding CSPMNs has focused on their formation only in tetrahydrofuran (THF)[5,8–16,23] and 1,4-dioxane.[18,19] According to Prat *et al.*,[26] these organic solvents are considered to be 'problematic' or 'hazardous' and they should be avoided, especially in cases where the synthesized polymers are intended to be used in biomedical applications, since they can affect their toxicity. It is worth mentioning here that there are only two reports in the literature where CSPMNs have been used for biomedical applications, and more specifically, for DNA adsorption,[10,12] whereas these well-defined polymeric nanostructures were not used before for drug encapsulation and delivery.

Star polymers,[27–31] which are the precursors of CSPMNs, consist of linear polymer chains (star polymer "arms") connected together at a central point called the "core". These branched polymeric nanostructures have been widely utilized

[a]*School of Chemistry and Chemical Engineering, Queen's University Belfast, David Keir Building, Belfast, BT9 5AG, UK. E-mail: e.themistou@qub.ac.uk*
[b]*Polymer Characterisation Research Technology Platform, University of Warwick, Library Road, Coventry, CV4 7AL, UK*

†Electronic supplementary information (ESI) available: Experimental section; additional ^{1}H NMR spectra; DLS, SEC, SLS and UV-vis data. See DOI: https://doi.org/10.1039/d3py00677h

in the biomedical field for various applications,[32] such as gene[33–42] and drug delivery.[43–45] Although in most synthetic procedures in the literature star polymers were prepared using organic solvents,[35,46–49] contrary to the CSPMNs, in some recent studies by our group[38] and other researchers, heterogeneous RAFT emulsion and dispersion polymerization in water or water/alcohol mixtures[50–57] was used to synthesize star polymers. This is a biologically friendly synthetic methodology, since only water and alcohols (reported as 'recommended' solvents that are good alternatives to organic solvents for the preparation of polymers[26]) are used. Another advantage of this aqueous synthetic procedure is that it is more efficient than RAFT polymerization in organic solvents since it can result in low dispersity ($Đ$) values and high yields with high solids content. Therefore, this synthetic methodology appears to be promising for the development of both biocompatible CSPMNs and their star polymer precursors.

The synthesis of CSPMNs using biologically friendly conditions, such as an aqueous solution at physiological temperature (37 °C), can immensely increase their potential biological applications. Although RAFT polymerization has been an ever more frequently used "living" controlled polymerization technique since its conception by researchers in CSIRO, Australia,[24,25] there are currently no reports in the literature on the synthesis of CSPMNs or "in–out" star polymers by aqueous RAFT polymerization. In our previous work, we investigated the formation of biocompatible cationic "arm-first" star polymers *via* aqueous RAFT polymerization.[38] In this work, we use a similar methodology for the preparation of more advanced nanostructures: "in–out" star polymers and their CSPMN derivatives.

Herein, in order to make sure that the resulting CSPMNs will have increased biocompatibility for use in biomedical applications and especially in drug delivery, both the neutral polyethylene glycol (PEG)-based monomer, OEGMA,[58] and the acid-labile diacetal-based bis[(2-methacryloyloxy)ethoxymethyl] ether (MOEME)[15,38,59] cross-linker were used. PEG is extensively used in biomedical applications[60] due to its high biocompatibility and OEGMA was used before for the preparation of CSPMNs[11] for use in biomedical applications. The use of MOEME produces CSPMNs with degradable cores[15] that can break down in acidic environments (such as tumors). Their low molecular weight (MW) degradation products can potentially be easily removed from the body through normal metabolic pathways. In more detail, the preparation of novel biocompatible PEG-based CSPMNs (star-based gels) with acid-labile diacetal MOEME-based and non-degradable ethylene glycol dimethacrylate (EGDMA)-based cores by a facile RAFT polymerization methodology under biologically friendly conditions, *i.e.* with water as polymerization solvent and physiological temperature (37 °C), is described here (see Scheme 1). The synthetic procedure involved four steps: synthesis of a linear polymer in ethanol by the addition of an OEGMA monomer to a mixture of solvent and polymerization initiator/agent (Scheme 1a), followed by the preparation of two different types of star polymers, "arm-first" and "in–out"[61] (Scheme 1b and c, respectively), and finally, the synthesis of the CSPMN (Scheme 1d)[5] in water at 37 °C. In more detail, the

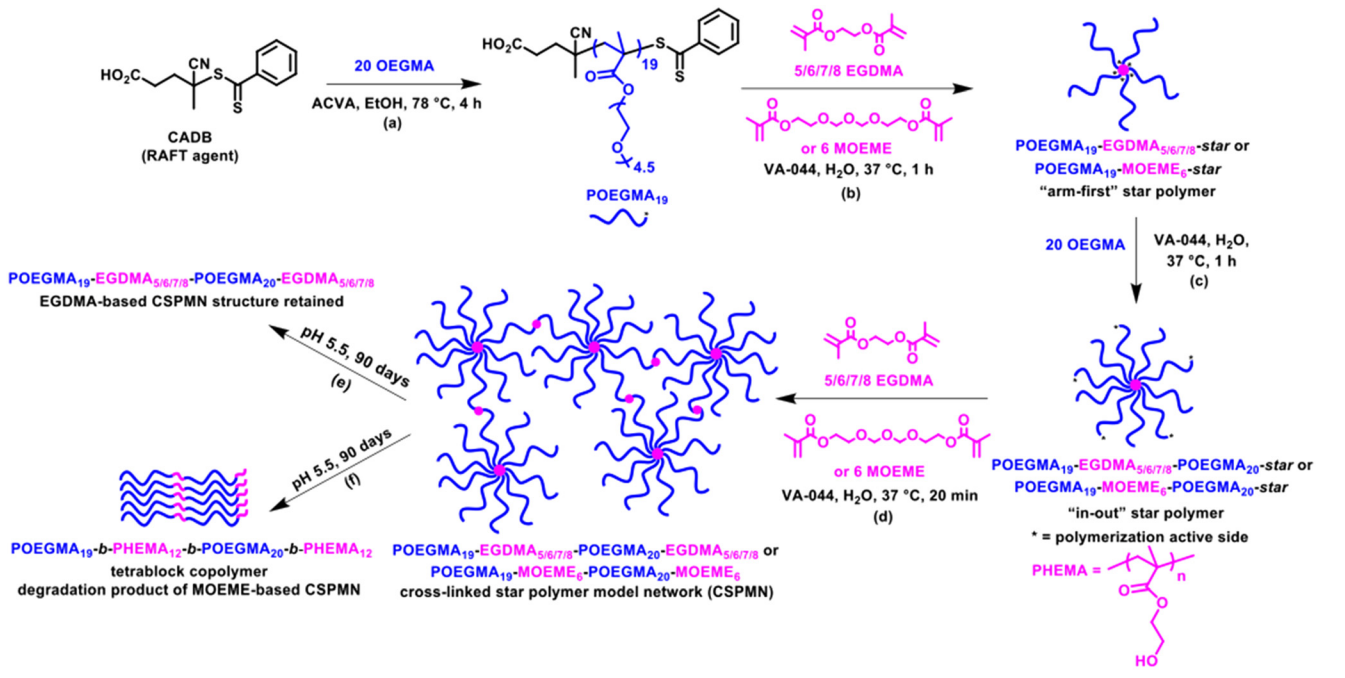

Scheme 1 Reaction scheme for the synthesis of the (a) macro-CTA by RAFT solution polymerization in ethanol, synthesis of (b) "arm-first" star polymers, (c) "in–out" star polymers and (d) CSPMNs by aqueous RAFT polymerization, and degradation trial for (e) EGDMA-based and (f) MOEME-based CSPMNs under acidic conditions.

first star polymer precursors were synthesized using the "arm-first" approach by the addition of a cross-linker to a linear POEGMA polymer (Scheme 1b). Subsequently, a second type of star polymer precursor was prepared using the "in–out" approach following the addition of more monomer to the "arm-first" star polymers (Scheme 1c). Then, the CSPMNs were formed by the addition of cross-linkers to the "in–out" star polymers (Scheme 1d). The polymerization conditions were optimized for the formation of the CSPMNs.

This preparation method of CSPMNs, which is based on "in–out" star polymer precursors,[16,19] was chosen here since it is considered to be better than the "core-first" type star polymer precursor method.[18] The "in–out" method can give less star–star coupling and better star polymer size homogeneity due to steric hindrance conferred by the star polymer arms prepared in the first polymerization step. Furthermore, multi-functional initiators or RAFT agents normally require more multi-step procedures as they are not usually commercially available. It is also possible to add different functionalities to "in–out" star polymers by using different monomers for the second arm formation and, depending on the desired application, this characteristic may be desirable. This can be exploited to add further functionality, such as the ability to conjugate to peptides for biomedical applications.[28]

The use of the acid-labile diacetal-based MOEME cross-linker (prepared using the procedure described by Themistou *et al.*[62]) for both the preparation of the "arm-first" (Scheme 1b) and the preparation of the CSPMN (Scheme 1d) resulted in the formation of a CSPMN that, contrary to the non-degradable EGDMA-based CSPMN (Scheme 1e) prepared by the commercially available EGDMA cross-linker, can degrade to a linear polymer under acidic conditions similar to the ones found in cancerous tumors (Scheme 1f). Finally, rhodamine B dye (used as a surrogate drug entity) encapsulation *in situ* during the synthesis of the MOEME-based CSPMN was performed followed by its release monitoring from the acid-labile CSPMN. To our knowledge, this is the first report on CSPMN and "in–out" star polymer synthesis in water and in physiological temperature. This is also the first encapsulation (during polymerization) and release study using a CSPMN.

Results and discussion

Preparation of the hydrophilic POEGMA macro-CTAs

The hydrophilic $POEGMA_{19}$ macro-chain transfer agent (macro-CTA) was prepared in ethanol at 78 °C for 4 h (Scheme 1a). This was performed using an OEGMA monomer with a short PEG chain (4–5 PEG units), as opposed to longer PEG chained OEGMA monomers, to minimize any steric hindrance issues in the incorporation of the POEGMA linear polymer arms to the star polymer core during the "arm-first" star polymer formation (Scheme 1b). The successful preparation of the macro-CTA was confirmed by proton nuclear magnetic resonance spectroscopy (^{1}H NMR) spectroscopy in deuterated chloroform ($CDCl_3$) and size exclusion chromatography (SEC) in THF. More specifically, a high monomer conversion of 97% was confirmed by ^{1}H NMR spectroscopy by comparing the area under the methacrylic peaks at 5.55 and 6.11 ppm with the area under the polymer/monomer peak at 4.07 ppm. This corresponds to a POEGMA macro-CTA with a mean degree of polymerization (DP) of 19 and a MW of 5979 g mol^{-1}. The purified $POEGMA_{19}$ macro-CTA (after dialysis using methanol), was characterized by ^{1}H NMR spectroscopy and its ^{1}H NMR characteristic peaks are shown in Fig. S1a.† The obtained SEC (THF) chromatogram of the macro-CTA (Fig. 1) showed a relatively narrow molecular weight distribution (MWD) with a $Đ$ value of 1.27. A number-average MW (M_n) value of 5110 g mol^{-1} and a peak molecular weight (weight at the peak maximum, M_p) value of 6780 g mol^{-1} were determined. The M_n value was in relatively good agreement with the ^{1}H NMR MW value. The slightly high $Đ$ value obtained is attributed to traces of EGDMA cross-linker impurity present in the commercially available OEGMA monomer.[38,63,64] This can cause some chain–chain coupling reactions during the formation of POEGMA, which were not found to significantly affect the subsequent "arm-first" polymer formation.[38]

Preparation of "arm-first" star polymers

In order to investigate the likelihood and efficacy of CSPMN formation, initially the POEGMA macro-CTA was reacted with either the degradable acid-labile MOEME or the non-degradable EGDMA cross-linker, to form star polymers (CSPMN precursors) using an "arm-first" approach[61,62,65] (Scheme 1b). These star polymers were synthesized by aqueous RAFT polymerization with a 25% w/w solids content at 37 °C over 1 h, the time required to reach full cross-linker conversion and maximum conversion of the arm into the star polymer. A series of non-degradable "arm-first" star polymers were prepared with varying EGDMA cross-linker : macro-CTA (5 : 1, 6 : 1, 7 : 1 and 8 : 1) molar ratios to optimize the amount of cross-linker used for the synthesis of CSPMNs and their "arm-first" and "in–out" star polymer precursors. The results of their

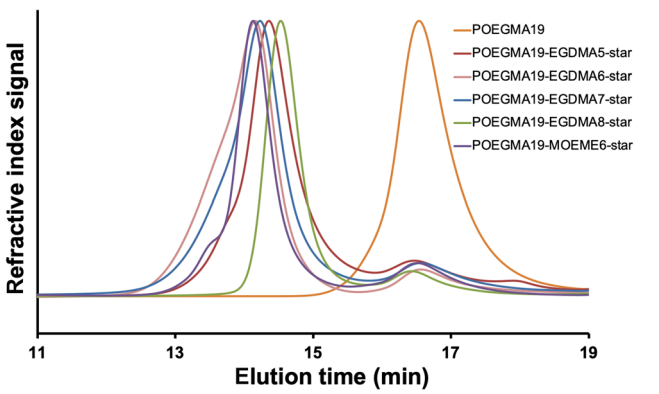

Fig. 1 SEC (THF) chromatograms of all POEGMA-EGDMA-*star* (EGDMA : macro-CTA molar ratios = 5 : 1, 6 : 1, 7 : 1, 8 : 1) and POEGMA-MOEME-*star* (MOEME : macro-CTA molar ratio = 6 : 1) "arm-first" star polymers and their linear POEGMA macro-CTA precursors.

Table 1 MWs, $Đ$ values, fraction of unattached arms (% linear polymer) and hydrodynamic diameters for the synthesized acid-labile and non-degradable POEGMA-based "arm-first" star polymers prepared *via* aqueous RAFT polymerization at 37 °C

Star polymer structure	M_n[a] [g mol^{-1}]	$Đ$ value[a]	% Linear polymer[a]	Hydrodynamic diameter[b] [nm]	Number of arms[c]
POEGMA$_{19}$-EGDMA$_5$-*star*	49 400	1.31	14.1	14.1	33
POEGMA$_{19}$-EGDMA$_6$-*star*	76 700	1.32	9.6	18.8	79
POEGMA$_{19}$-EGDMA$_7$-*star*	65 200	1.45	13.6	18.7	39
POEGMA$_{19}$-EGDMA$_8$-*star*	115 200	1.12	8.4	21.5	78
POEGMA$_{19}$-MOEME$_6$-*star*	70 800	1.23	17.0	12.3	27

[a] Data obtained by THF SEC *versus* PMMA standards. [b] Data obtained by DLS in water (intensity-average diameter distribution). [c] Data obtained by SLS.

characterization by SEC and static light scattering (SLS) are presented in Table 1. Dynamic light scattering (DLS) data are presented in Table 1 and Fig. S2† and ^{1}H NMR ($CDCl_3$) data are shown in Fig. S7–S10.†

The SEC (THF) chromatograms of the "arm-first" star polymers, overlaid in Fig. 1 together with their POEGMA macro-CTA linear polymer precursor, showed that a shift to lower elution times was observed when compared to their respective macro-CTA, indicative of an increase in MW due to the interconnection of the linear polymer arms to the cross-linker core and successful formation of the star-shaped polymers. The SEC data presented in Table 1, also shows that the "arm-first" star polymers have much higher M_n values (49 400–115 200 g mol^{-1}) than the macro-CTA (5110 g mol^{-1}). Their light scattering M_w values were used to give an indication of the approximate number of arms in each star polymer (Table 1). The number of arms was calculated as the star polymer light scattering M_w value after subtracting the cross-linker contribution (number of cross-linker units multiplied by the cross-linker MW) divided by the light scattering M_w of the POEGMA macro-CTA. All light scattering M_w values are provided in Table S1.† A small amount (8–17%) of unreacted linear polymer precursors is still present in all reaction products after the synthesis of the "arm-first" star polymer, which is common in "arm-first" RAFT polymerization.[38,55,66] This is also evident in the SEC chromatograms of all the star polymers (Fig. 1), where the MWD appeared to be bimodal. The higher peak that appears at the lower elution time corresponds to the star polymer, while the small peak appearing at around 16 to 17 min elution time is due to the remaining linear polymer that was not attached to the star polymer core. The areas under the two peaks in the chromatogram were used to calculate the % unreacted linear polymer (8–17%, Table 1). These values were relatively low compared to others in the literature and therefore purification of the star polymers was deemed unnecessary and was avoided to minimize product loss. The $Đ$ values of the "arm-first" star polymers were found to range from 1.12 to 1.45 for the EGDMA-based star polymers. The MOEME-based star polymer had a $Đ$ value of 1.23. These relatively low values for "arm-first" star polymer formation compared to previous studies[59,62,67,68] suggest that well-defined star polymers were formed, which was also evident by the hydrodynamic diameter values obtained for all the "arm-first" star polymers, ranging

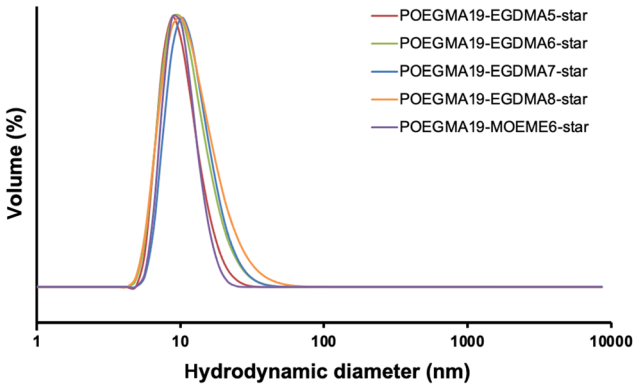

Fig. 2 DLS volume weighted diameter distribution for all "arm-first" POEGMA$_{19}$-EGDMA$_x$-*star* and POEGMA$_{19}$-MOEME$_y$-*star* star polymers (1 mg mL^{-1} in deionized water).

from 12 to 22 nm (Fig. 2 and Table 1). The POEGMA$_{19}$-EGDMA$_8$-*star* appeared to have the highest hydrodynamic diameter (22 nm) while POEGMA$_{19}$-MOEME$_6$-*star* had the lowest hydrodynamic diameter (12 nm).

For the EGDMA-containing "arm-first" star polymers, it was found that the cross-linker : macro-CTA molar ratio of 8 : 1 was the most efficient for star polymer formation as it yielded the lowest % linear polymer (8.4%), the lowest $Đ$ value (1.12) and the highest M_n value (115 200 g mol^{-1}) when compared to the other molar ratios used (5 : 1, 6 : 1 and 7 : 1). On the other hand, the 5 : 1 molar ratio gave the highest % linear polymer (14.1%) for the EGDMA-based star polymers, which meant that POEGMA$_{19}$-EGDMA$_5$-*star* was excluded from the experiments that followed for the synthesis of "in–out" star polymers and CSPMNs. Additionally, POEGMA$_{19}$-EGDMA$_5$-*star* and POEGMA$_{19}$-EGDMA$_7$-*star* had a larger % linear polymer in their samples, which led to them having fewer attached arms than POEGMA$_{19}$-EGDMA$_6$-*star* and POEGMA$_{19}$-EGDMA$_8$-*star* that exhibited a smaller % linear polymer through SEC. The EGDMA : macro-CTA molar ratio of 7 : 1 also appeared to give a high % linear polymer (13.6%) and the highest $Đ$ value (1.45) of all the EGDMA "arm-first" star polymers prepared, with a number of arms of 39. A general trend was observed whereby the number of arms increased as the EGDMA : macro-CTA molar ratio increased, with POEGMA$_{19}$-EGDMA$_6$-*star* having

Table 2 Solids content, MWs, $Đ$ values, fraction of unattached arms (% linear polymer) and hydrodynamic diameters for the synthesized "in–out" star polymers *via* aqueous RAFT polymerization at 37 °C

Star polymer structure	% Solids content (w/w)	OEGMA % conversion	M_n[a] [g mol^{-1}]	$Đ$ value[a]	% Linear polymer[a]	Hydrodynamic diameter[b] [nm]	Number of arms[c]
POEGMA$_{19}$-EGDMA$_6$-POEGMA$_{20}$-*star*	10	97.6	122 400	1.96	6.2	41.2	69
POEGMA$_{19}$-EGDMA$_7$-POEGMA$_{20}$-*star*	25	∼100.0	149 900	2.77	13.9	48.6	107
POEGMA$_{19}$-EGDMA$_7$-POEGMA$_{20}$-*star*	10	97.7	106 900	2.32	6.5	55.8	63
POEGMA$_{19}$-EGDMA$_8$-POEGMA$_{20}$-*star*	10	99.3	315 800	2.01	4.4	230.1	89
POEGMA$_{19}$-MOEME$_6$-POEGMA$_{20}$-*star*	25	98.1	104 700	1.77	8.3	23.9	42
POEGMA$_{19}$-MOEME$_6$-POEGMA$_{20}$-*star*	10	∼100.0	75 700	1.42	6.4	25.1	30

[a] Data obtained by THF SEC *versus* PMMA standards. [b] Data obtained by DLS in water (intensity-average diameter distribution). [c] Data obtained by SLS.

the most arms (79) although there is a shoulder peak evident in its SEC chromatogram (Fig. 1), which may contribute to this high value and large light scattering MWs (Table S1†). All EGDMA star polymers had a larger number of arms than POEGMA$_{19}$-MOEME$_6$-*star* (27). However, in subsequent experiments, the 8 : 1 molar ratio resulted in aggregation in the "in–out" star polymer synthesis (aggregates of around 230 nm were observed based on DLS measurements, Table 2), while the formation of CSPMNs (in 10% w/w or 25% w/w solids content) was not successful. Therefore, an EGDMA cross-linker : macro-CTA molar ratio of 6 : 1, with a relatively good % linear polymer of 9.6% and a $Đ$ value of 1.32, was considered to be the optimum for the synthesis of a non-degradable EGDMA-based CSPMN. This cross-linker : macro-CTA molar ratio was also used for the preparation of the acid-labile CSPMN using the acid-labile MOEME cross-linker.

Similarly, a core degradable "arm-first" POEGMA$_{19}$-MOEME$_6$-*star* star polymer was synthesized to be used as a precursor for the synthesis of a core degradable "in–out" star polymer and a core degradable CSPMN. The successful preparation of this "arm-first" star polymer is evidenced by the presence of the diacetal protons of the MOEME cross-linker at 4.81 ppm in its ^{1}H NMR ($CDCl_3$) spectrum (Fig. S1b and S11†). The two "arm-first" star polymers prepared using a molar ratio of 6 : 1 and the two different cross-linkers (EGDMA and MOEME) appeared to have similar SEC M_n values (76 700 and 70 800 g mol^{-1}, respectively). However, POEGMA$_{19}$-EGDMA$_6$-*star* yielded a higher number of arms (79) than POEGMA$_{19}$-MOEME$_6$-*star* (27). As also shown in our previous work,[38] the bulkier, degradable MOEME cross-linker is not as efficient as the non-degradable EGDMA cross-linker in forming "arm-first" star polymers, with the % unreacted linear polymer for POEGMA$_{19}$-MOEME$_6$-*star* of 17.0% compared to 9.6% for its corresponding POEGMA$_{19}$-EGDMA$_6$-*star*. However, although the EGDMA cross-linker appeared to be better in incorporating linear polymer chains to the star polymer core, the MOEME cross-linker gave a more uniform star polymer with a lower $Đ$ value (1.23 compared to 1.32 for EGDMA). Furthermore, in the subsequent "in–out" star polymer synthesis, the MOEME star polymer was found to be more efficient and successful in two concentrations (10% and 25% w/w) compared with one for the EGDMA star polymer (10% w/w).

Further investigation of the DLS data (Table 1) of the EGDMA-based "arm-first" star polymers shows a general trend of an increase in the hydrodynamic diameter with a general increase in the amount of cross-linker used in the star polymer synthesis and/or an increase in the number of arms incorporated in the star polymer (from 14 nm for the star polymer with a 5 : 1 cross-linker : macro-CTA molar ratio with only 33 arms to 22 nm for the one with an 8 : 1 molar ratio with 78 arms). The other two "arm-first" star polymers (6 : 1 and 7 : 1 ratios) have intermediate hydrodynamic diameter values. More specifically, POEGMA$_{19}$-EGDMA$_6$-*star* with a 6 : 1 ratio and 79 arms appeared to have a similar hydrodynamic diameter (18.8 nm) to the POEGMA$_{19}$-EGDMA$_7$-*star* with a 7 : 1 ratio and 39 arms (18.7 nm). These results suggest that an increase in the amount of cross-linker can give a higher hydrodynamic diameter for the "arm-first" star polymer, due to a larger core and/or a higher number of arms attached to the core resulting in the chains being more extended.

Since the POEGMA$_{19}$-MOEME$_6$-*star* and POEGMA$_{19}$-EGDMA$_6$-*star* appeared to have a similar increase in MW with comparatively good $Đ$ values (1.23 and 1.32, respectively), they were selected as the best candidates for "in–out" star polymer and CSPMN syntheses.

Preparation of "in–out" star polymers

After optimizing the preparation of "arm-first" star polymers, an addition of more OEGMA monomers resulted in the formation of new arms growing from the center (core) of the star polymers and therefore, an increase in the MW of the star polymers, resulting in what is known as "in–out" star polymers (Scheme 1c).[61,69,70] The "living" character of the polymer chain facilitates this step as the polymerization active sites are on the core of the "arm-first" star polymers. Therefore, the newly formed POEGMA linear chains emanate from the core.

Initially, two kinetic studies were conducted for the synthesis of POEGMA$_{19}$-EGDMA$_7$-POEGMA$_{20}$-*star* at 37 °C using two different % solids content values (25% w/w and 10% w/w). Samples were taken at different time points (every hour) over a course of 4 hours to study the effect of reaction time on "in–out" star polymer formation. From these experiments, it was found that for both % solids content values, a reaction time of 1 h was sufficient for the formation of the "in–out" star

polymer, since lower $Đ$ values were obtained (Table S2†) in 1 h, while the molecular weight was not changed significantly by increasing the reaction time. By comparing the two different % solids content values, it was concluded that 10% w/w was more favorable for the formation of the EGDMA-based "in–out" POEGMA$_{19}$-EGDMA$_7$-POEGMA$_{20}$-*star* due to the lower $Đ$ value (2.32 compared to 2.77 for the 25% w/w) obtained for the 1 hour reaction time.

Following the kinetic studies, a series of non-degradable "in–out" POEGMA$_{19}$-EGDMA$_x$-POEGMA$_{20}$-*star* polymers (where x = 6, 7, and 8) and the acid-labile "in–out" POEGMA$_{19}$-MOEME$_6$-POEGMA$_{20}$-*star* star polymers were prepared using their corresponding synthesized "arm-first" star polymer precursors (^{1}H NMR ($CDCl_3$) spectra shown in Fig. S12–S17†). All EGDMA-based "in–out" star polymers were prepared using 10% w/w solids content, as this was found to give more uniform star polymers based on the results of the kinetic studies and the formation of a POEGMA$_{19}$-EGDMA$_6$-POEGMA$_{20}$-*star* chemical gel at 25% w/w concentration. For the MOEME-based POEGMA$_{19}$-MOEME$_6$-POEGMA$_{20}$-*star* both 10% w/w and 25% w/w solids contents were used. As an example, the ^{1}H NMR characteristic peaks for the "in–out" POEGMA$_{19}$-MOEME$_6$-POEGMA$_{20}$-*star*, a precursor of the MOEME-based CSPMN, are shown in Fig. S1c†, and they indicate the successful incorporation of the POEGMA arms in the "arm-first" star polymer core to form the "in–out" star polymer. Table 2 shows the % solids contents, % OEGMA monomer conversions, MWs, $Đ$ values and % unattached linear polymer values obtained by SEC (THF), hydrodynamic diameters determined by DLS (Fig. S3†) and the total number of arms by SLS for these "in–out" star polymers.

The % OEGMA monomer conversions were very high (97.6–100%) for all "in–out" star polymers, indicating that the reaction time used (1 h) was sufficient to polymerize almost all of the OEGMA monomer. This corresponds to a DP value of 20 for the new POEGMA$_{20}$ chains that grew out from the "arm-first" star polymer core in this polymerization step. To calculate how many new POEGMA chains were created in this polymerization step, the light scattering M_w value of their corresponding "arm-first" star polymer precursors was subtracted from the light scattering M_w value of the "in–out" star polymer and the obtained value was divided by the light scattering M_w value of the POEGMA$_{19}$ macro-CTA. Then to find the total number of arms in the "in–out" star polymer (Table 2) the new number of arms found by this calculation was added to the number of arms of the "arm-first" star polymer (Table 1). The SEC (THF) data for all of these "in–out" star polymers showed a lower elution time compared to both their linear and "arm-first" star polymer precursors, as observed in Fig. 3, indicating the successful formation of "in–out" star

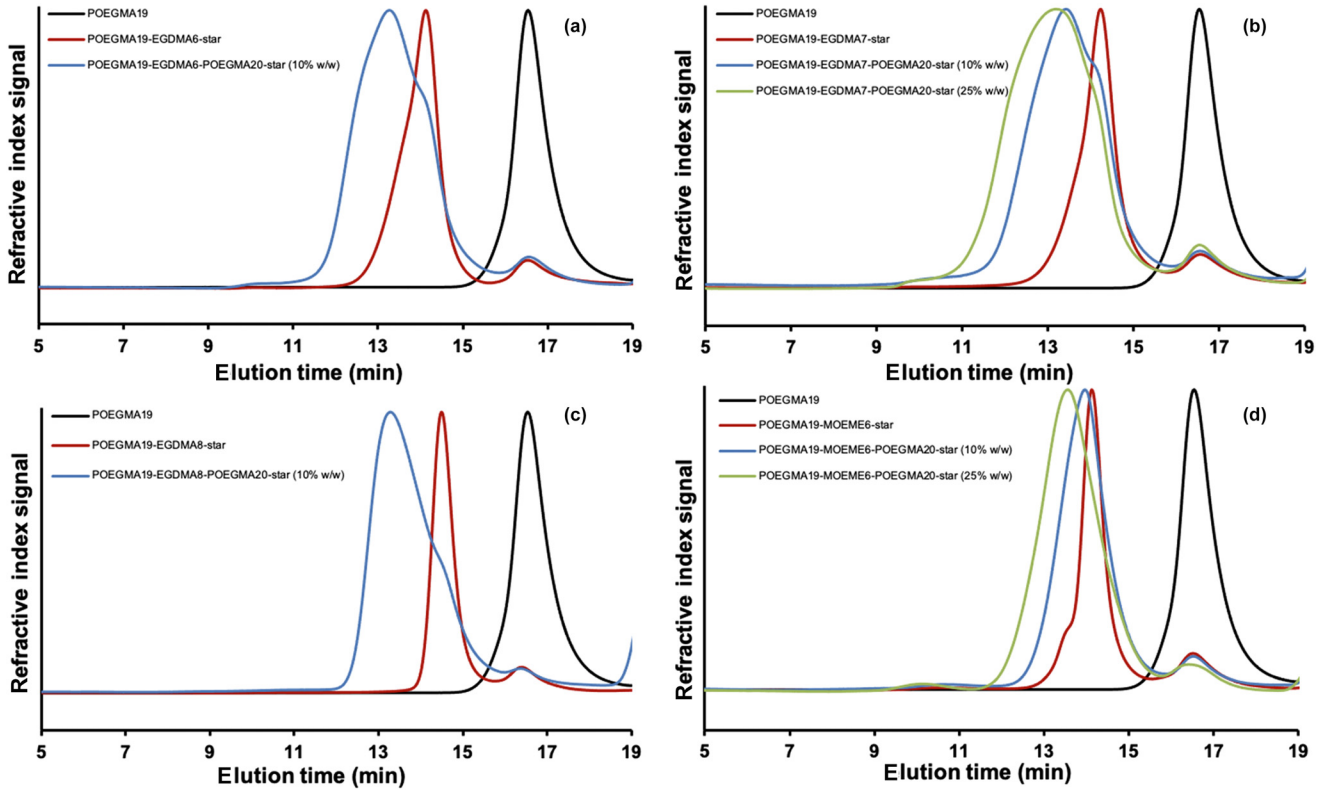

Fig. 3 SEC (THF) chromatograms showing the synthesis (macro-CTA, "arm-first" star polymers, and "in–out" star polymers) of (a) POEGMA$_{19}$-EGDMA$_6$-POEGMA$_{20}$-*star*, (b) POEGMA$_{19}$-EGDMA$_7$-POEGMA$_{20}$-*star*, (c) POEGMA$_{19}$-EGDMA$_8$-POEGMA$_{20}$-*star* and (d) POEGMA$_{19}$-MOEME$_6$-POEGMA$_{20}$-*star* "in–out" star polymers.

polymers. As expected, the M_n values of the "in–out" star polymers (75 700–149 900 g mol^{-1}) and their $Đ$ values (1.42–2.77) were higher than the ones of their corresponding "arm-first" star polymer precursors (70 800–115 200 g mol^{-1} and 1.12–1.45, respectively), while the calculated % linear polymer values (4.4–13.9) are lower than the calculated "arm-first" star polymer values (8.4–17.0). It is interesting to mention here that both MOEME-based "in–out" star polymers yielded much lower $Đ$ values (1.42–1.77) than their EGDMA-based equivalents (1.96–2.77). When EGDMA was used as a cross-linker a number of issues arose with "in–out" star polymer formation. POEGMA$_{19}$-EGDMA$_6$-POEGMA$_{20}$-*star* yielded fewer arms from SLS (69) when compared to its POEGMA$_{19}$-EGDMA$_6$-*star* precursor (79) and this can be attributed to a large number of "arm-first" star polymers present in this sample. This can be observed as a shoulder peak around 14.5 min in its SEC chromatogram (Fig. 3(a)) and suggests that the formation of POEGMA$_{19}$-EGDMA$_6$-POEGMA$_{20}$-*star* is inefficient. Similarly, the formation of POEGMA$_{19}$-EGDMA$_7$-POEGMA$_{20}$-*star* in 25% w/w solids concentration yielded 107 arms, which is more than double the number of arms of its star polymer precursor (39) and suggests an inefficient star preparation (possibly due to star–star coupling) as the number of arms in the "in–out" star polymer cannot be more than double that of its "arm-first" star polymer precursor. The large light scattering MW values observed (Table S1†) are likely a result of the wide MWD observed by SEC (Fig. 3(b)). When POEGMA$_{19}$-EGDMA$_7$-POEGMA$_{20}$-*star* was synthesized in 10% w/w solids concentration the number of arms observed was 63, further adding credence to our observation that 10% w/w is a more suitable concentration for the synthesis of EGDMA "in–out" star polymers. This difference is also seen in their SEC chromatograms where POEGMA$_{19}$-EGDMA$_7$-POEGMA$_{20}$-*star* has a narrower MWD in 10% w/w compared to 25% w/w. The synthesis of POEGMA$_{19}$-EGDMA$_8$-POEGMA$_{20}$-*star* yielded a small increase in the number of arms (from 78 to 89) although its synthesis was shown to result in aggregation as determined by DLS. When MOEME was used as a cross-linker, as also found with the EGDMA-based star polymers, the more dilute reaction mixture (10% w/w solids content) gives more uniform POEGMA$_{19}$-MOEME$_6$-POEGMA$_{20}$-*star* star polymers with lower $Đ$ values: 1.42 for the 10% w/w compared to 1.77 for the 25% w/w solids content. However, the reaction for the synthesis of the POEGMA$_{19}$-MOEME$_6$-POEGMA$_{20}$-*star* using 10% w/w solids content did not appear to work well, since the M_n value (75 700 g mol^{-1}) of the resulting "in–out" star polymer (Table 2) was only slightly higher than its "arm-first" star polymer precursor (70 800 g mol^{-1}), as shown in Table 1. Light scattering data also indicated that only 3 extra arms were attached to POEGMA$_{19}$-MOEME$_6$-POEGMA$_{20}$-*star* (30) compared to POEGMA$_{19}$-MOEME$_6$-*star* (27). On the other hand, when 25% w/w solids content was used for the POEGMA$_{19}$-MOEME$_6$-POEGMA$_{20}$-*star* synthesis, a higher M_n value (104 700 g mol^{-1}) was determined and more arms were observed (42), showing that this higher solids content is more efficient in this synthetic step. These results suggest that

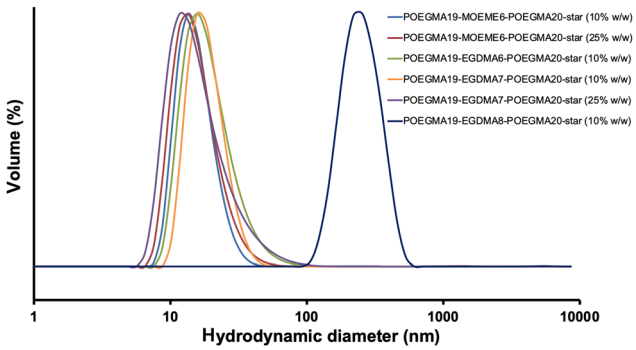

Fig. 4 DLS volume weighted diameter distribution for all "in–out" POEGMA$_{19}$-EGDMA$_x$-POEGMA$_{20}$-*star* and POEGMA$_{19}$-MOEME$_y$-POEGMA$_{20}$-*star* star polymers (1 mg mL^{-1} in deionized water).

MOEME is a better cross-linker to use for preparing these star polymers as it yields more desirable values from SEC and SLS.

The DLS volume data for all the synthesized "in–out" star polymers are presented in Fig. 4 and their hydrodynamic diameters (based on intensity) are shown in Table 2. All "in–out" star polymers appeared to have hydrodynamic diameters in the range of 23.9–55.8 nm except for the POEGMA$_{19}$-EGDMA$_8$-POEGMA$_{20}$-*star* (10% w/w), which has a noticeably higher hydrodynamic diameter, possibly due to some star–star polymer coupling or formation of star polymer aggregates due to the high amount of cross-linker used for its preparation. These hydrodynamic diameters were higher than the ones determined for the "arm-first" star polymers (12.3–21.5 nm). The % solids content used in the synthesis of the "in–out" star polymers does not seem to significantly affect their hydrodynamic diameter. More specifically, POEGMA$_{19}$-MOEME$_6$-POEGMA$_{20}$-*star* and POEGMA$_{19}$-EGDMA$_7$-POEGMA$_{20}$-*star* were found to have similar hydrodynamic diameters at both 10% and 25% w/w solids content. POEGMA$_{19}$-MOEME$_6$-POEGMA$_{20}$-*star* had a hydrodynamic diameter of 24 nm at 10% w/w compared to 25 nm at 25% w/w, while POEGMA$_{19}$-EGDMA$_7$-POEGMA$_{20}$-*star* appeared to have higher hydrodynamic diameters: 56 nm at 10% w/w and 49 nm at 25% w/w. As shown in Table 2, the degradable MOEME cross-linker resulted in the formation of "in–out" star polymers with smaller (24–25 nm) hydrodynamic diameters than those of EGDMA (41–230 nm), consistent with smaller MWs. For the EGDMA-based "in–out" star polymers, the higher amount of cross-linker used during the synthesis, the higher was the observed star polymer hydrodynamic diameter.

Preparation of CSPMNs

After the synthesis of the "in–out" star polymers, where the polymerization active sites are on the ends of the newly prepared polymer arms, at the periphery of the star polymers, attempts were made to prepare cross-linked star polymer gels (CSPMNs[5]). The synthesis of the CSPMNs was investigated by adding more cross-linker to connect the "in–out" star polymers together, as can be seen in Scheme 1d, and observing if gela-

tion occurred. Based on the results presented above for the synthesis of the star polymers, the best "in–out" star polymers for the synthesis of core degradable and non-degradable CSPMNs are the ones with a cross-linker : macro-CTA molar ratio of 6 : 1, namely the non-degradable POEGMA$_{19}$-EGDMA$_6$-POEGMA$_{20}$-*star* and the core degradable POEGMA$_{19}$-MOEME$_6$-POEGMA$_{20}$-*star*. The synthesized CSPMNs were hydrophilic as they were prepared using the PEG-based methacrylic monomer OEGMA, so that they can be used in biomedical applications.[11] Gelation, which indicates successful formation of the CSPMN, was obtained for the non-degradable POEGMA$_{19}$-EGDMA$_6$-POEGMA$_{20}$-EGDMA$_6$ at 10% w/w solids content and the core degradable POEGMA$_{19}$-MOEME$_6$-POEGMA$_{20}$-MOEME$_6$ at 25% w/w solids content (Fig. S4†).

The SEC data of the CSPMN star polymer precursors (Fig. 1 and 3, Tables 1 and 2) indicate that only a small amount of unattached linear polymer is present at the end of their synthesis. More specifically, the non-degradable "arm-first" POEGMA$_{19}$-EGDMA$_6$-*star* and the core degradable POEGMA$_{19}$-MOEME$_6$-*star* star polymers had 9.6% and 17.0% unattached linear polymer (Table 1), respectively. The non-degradable "in–out" POEGMA$_{19}$-EGDMA$_6$-POEGMA$_{20}$-*star* (10% w/w solids content) and the core degradable "in–out" POEGMA$_{19}$-MOEME$_6$-POEGMA$_{20}$-*star* (25% w/w solids content) appeared to have only 6.2% and 8.3% unattached linear polymer (Table 2), respectively. Therefore, purification was deemed unnecessary and was not performed in order to simplify the synthetic procedure and to avoid product loss. Also, a very small amount of OEGMA monomer is present at the end of the "in–out" star polymer reaction, 2.4% (97.6% conversion, Table 2) for the non-degradable "in–out" POEGMA$_{19}$-EGDMA$_6$-POEGMA$_{20}$-*star* (10% w/w solids content) and 1.9% (98.1% conversion, Table 2) for the core degradable "in–out" POEGMA$_{19}$-MOEME$_6$-POEGMA$_{20}$-*star* (25% w/w solids content). Both the small amounts of POEGMA linear polymer and OEGMA monomer present in the "in–out" star polymer precursors did not appear to impede the formation of the CSPMNs.

The formation of the non-degradable POEGMA$_{19}$-EGDMA$_6$-EGDMA$_{20}$-MOEME$_6$ CSPMN at 10% w/w solids content was quick as gelation time was only 20 min at 37 °C. However, when CSPMN formation for POEGMA$_{19}$-MOEME$_6$-POEGMA$_{20}$-MOEME$_6$ was attempted with 10% w/w solids content, gelation did not occur even after 48 h. The solution was possibly too dilute for the MOEME CSPMN to form, while also it is possible that the formation of the "in–out" POEGMA$_{19}$-MOEME$_6$-POEGMA$_{20}$-*star* star polymer in the previous step was incomplete (as discussed above). Therefore, CSPMN formation was carried out for POEGMA$_{19}$-MOEME$_6$-POEGMA$_{20}$-MOEME$_6$ using the 25% w/w "in–out" POEGMA$_{19}$-MOEME$_6$-POEGMA$_{20}$-*star* precursor. This yielded a CSPMN with a gelation time of only 20 min at 37 °C. The extractables from the CSPMN POEGMA$_{19}$-MOEME$_6$-POEGMA$_{20}$-MOEME$_6$ were collected and analyzed by SEC (THF) (Fig. S5†). The M_n, M_p and $Đ$ values of the two extractables' peaks determined by SEC (THF) were 29 630 g mol^{-1}, 28 170 g mol^{-1} and 1.38, respectively, for the peak at the lower elution time in the chromatogram. The same values were 6450 g mol^{-1}, 3230 g mol^{-1} and 1.68, respectively, for the peak at the higher elution time. The peak at the higher elution time is likely unreacted POEGMA$_{19}$, due to their similar M_p value. The peak at the lower elution time is theorized to be the result of an extension of the unreacted linear polymer present in the sample. The unreacted POEGMA$_{19}$ linear polymer will polymerize further with the excess OEGMA monomer added in the "in–out" star polymer synthetic step yielding linear polymers with a higher DP and larger MWs than the POEGMA$_{19}$ macro-CTA.

Degradation of CSPMNs under acidic conditions

The POEGMA$_{19}$-EGDMA$_6$-POEGMA$_{20}$-EGDMA$_6$ CSPMN is not degradable since it contains non-degradable EGDMA cross-links; therefore, it retains its structure under acidic conditions (Scheme 1e). On the contrary, the POEGMA$_{19}$-MOEME$_6$-POEGMA$_{20}$-MOEME$_6$ CSPMN has both primary (formed during the "arm-first" synthesis, Scheme 1b) and secondary (formed during the CSPMN synthesis, Scheme 1d) degradable diacetal-based MOEME cores. The acetals in the CSPMN cores can break down under acidic conditions[15,38,59,62,71–74] similar to the ones found in tumors (*i.e.* pH 5.5),[75] transforming the CSPMN structure to linear polymers,[15] with each unit of MOEME cross-linker giving two 2-hydroxyethyl methacrylate (HEMA) units. The degradation of the cross-linker, and therefore the CSPMN cores, eliminates the interconnection between the linear chains that are holding the CSPMN structure together and this results in the collapse of the network. As presented schematically in Scheme 1f, after the full degradation (90 days) of the POEGMA$_{19}$-MOEME$_6$-POEGMA$_{20}$-MOEME$_6$ CSPMN, its degradation product should be a POEGMA$_{19}$-*b*-PHEMA$_{12}$-*b*-POEGMA$_{20}$-*b*-PHEMA$_{12}$ tetrablock copolymer. The ^{1}H NMR ($CDCl_3$) spectrum of the degradation product is presented in Fig. S1d,† together with the linear POEGMA$_{19}$ (Fig. S1a†), "arm-first" POEGMA$_{19}$-MOEME$_6$-*star* (Fig. S1b†) and "in–out" POEGMA$_{19}$-MOEME$_6$-POEGMA$_{20}$-*star* (Fig. S1c†) CSPMN precursors. The HEMA oxymethylene proton peaks appear in the ^{1}H NMR ($CDCl_3$) spectrum of the degradation product at ~4.2 ppm (Fig. S1d†). The M_n, M_p and $Đ$ values of one of the CSPMN degradation products determined by SEC (THF) were 6720 g mol^{-1}, 7050 g mol^{-1} and 1.51, respectively, with the SEC trace shown in Fig. 5. These MW values are slightly higher than those of the linear POEGMA$_{19}$ (M_n = 5110 g mol^{-1} and M_p = 6780 g mol^{-1}), indicating that the degradation was successful since a linear polymer, which is longer than the initial linear POEGMA precursor, was obtained from the collapse of the CSPMN structure. There is a shoulder peak, present at a lower elution time, in the SEC trace of the degradation product with M_n, M_p and $Đ$ values of 20 120 g mol^{-1}, 10 720 g mol^{-1} and 1.41, respectively.

Encapsulation of rhodamine B dye within an acid-labile MOEME-based CSPMN

Once the most favorable conditions for the formation of an acid labile CSPMN were optimized (25% w/w, 37 °C), encapsu-

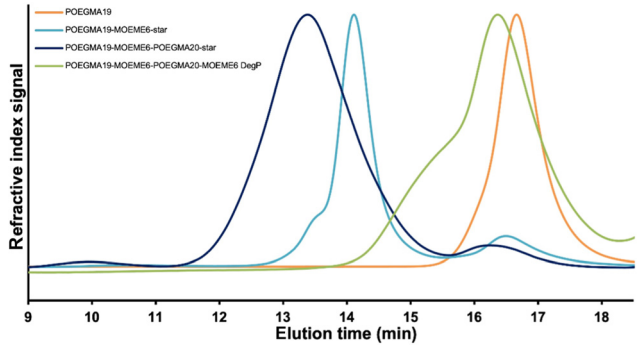

Fig. 5 SEC (THF) trace for the degradation product (DegP) of the $POEGMA_{19}$-$MOEME_6$-$POEGMA_{20}$-$MOEME_6$ CSPMN. Also included for comparison are the SEC (THF) traces of the precursors to $POEGMA_{19}$-$MOEME_6$-$POEGMA_{20}$-$MOEME_6$.

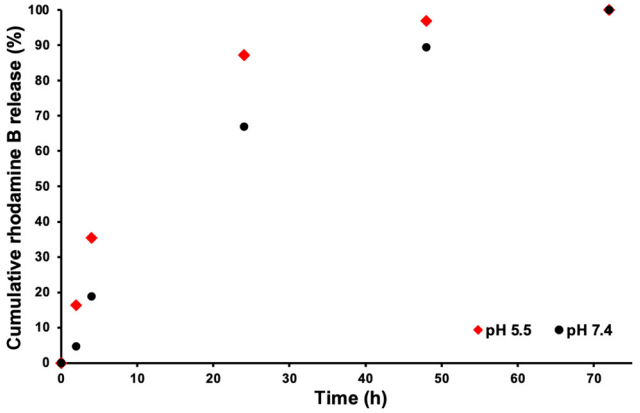

Fig. 6 % Cumulative rhodamine B release profile for the $POEGMA_{19}$-$MOEME_6$-$POEGMA_{20}$-$MOEME_6$ CSPMN in physiological pH (7.4) and acidic pH (5.5) at 37 °C over a period of 72 h.

lation of a drug model was performed *in situ* during the synthesis of the CSPMN. Since the polymerization reaction takes place under physiological conditions (aqueous solution, 37 °C), developing a methodology to encapsulate a biologically important molecule *in situ* during polymerization is very important for biomedical applications, and especially for drug delivery. This was tested here during the synthesis of the $POEGMA_{19}$-$MOEME_6$-$POEGMA_{20}$-$MOEME_6$ CSPMN using rhodamine B as a surrogate drug. The addition of the dye in the polymerization mixture for the CSPMN synthesis did not seem to affect the polymerization, since a gel was formed and the gelation time was the same as with the polymerization reaction without the dye (20 min). At the end of the polymerization, the dye was encapsulated (entrapped) in the CSPMN nanostructure, giving an intense pink color to the formed gel.

Release kinetics of rhodamine B from MOEME-based CSPMN

In order to mimic the conditions inside the body for drug release, two different dye release experiments were set up. One dye release study of the rhodamine B loaded $POEGMA_{19}$-$MOEME_6$-$POEGMA_{20}$-$MOEME_6$ CSPMN was conducted in a pH 7.4 buffer in order to mimic the physiological conditions while the other was conducted in a pH 5.5 buffer to imitate the pH of a cancerous late stage tumor.[75] The drug release was monitored over a period of a few days and samples were taken at various timepoints. The absorbance of the samples was measured using UV-vis spectroscopy (wavelength range 510–590 nm) and calibration curves were prepared for rhodamine B release in both pH 5.5 and pH 7.4 solutions (Fig. S6†). At around 72 h the fluorescence signal reached its maximum value in both pH values, therefore almost all of the amount of the rhodamine B dye that could be released from the CSPMN was transferred to its surrounding environment (7.80 μg for pH 7.4 and 2.99 μg for pH 5.5). Numerous studies have been carried out on how lower pH environments affect the structure and make-up of rhodamine B. It has been shown that not only do acidic environments protonate and alter the maximum UV wavelength absorbance of the dye but they also degrade rhodamine through protonation.[76–78] This goes someway to explaining the difference in the calculated amount of rhodamine released between the two pH environments (probably underestimated at pH 5.5). The color of each solution upon completion of the study is shown in Fig. S4.† A % cumulative release profile of rhodamine B for $POEGMA_{19}$-$MOEME_6$-$POEGMA_{20}$-$MOEME_6$ CSPMN in both pH 5.5 and pH 7.4 was constructed to observe the release of rhodamine B over time (with fluorescence maximum signal at 100%) and it is presented in Fig. 6. The release profiles of the rhodamine B encapsulated MOEME-based CSPMN show that the release rate decreased gradually during the period of 72 h at both pH values. At pH 5.5, a higher release rate was observed consistently over this period, which is attributed to some degradation of the CSPMN cores under these acidic conditions.

Conclusions

The preparation of well-defined polymeric networks under biologically friendly conditions has great potential in the biomedical field and especially in drug encapsulation and delivery. In this work, PEG-based CSPMNs with both acid-labile diacetal MOEME cores and non-degradable EGDMA cores were synthesized by aqueous RAFT polymerization at 37 °C from their linear, "arm-first" and "in–out" star polymer precursors. The successful formation of the CSPMNs was confirmed by facile gelation (in only 20 min). Both the core degradable and non-degradable CSPMNs, and their star polymer precursors, were of high quality, comparable with those synthesized previously in organic solvents. *In situ* encapsulation of rhodamine B in the acid-labile MOEME-based CSPMN was successful and dye release was observed by UV-vis. In conclusion, CSPMN formation using a biologically friendly aqueous RAFT polymerization approach was successful, and it presents a facile method of forming these acid-labile well-defined networks in a biologically friendly medium, which is desirable for drug delivery and other biomedical applications.

Data availability

The data supporting this article have been included as part of the ESI.†

Conflicts of interest

There are no conflicts to declare.

Acknowledgements

The authors acknowledge the Department for the Economy (DfE) for funding the Ph.D. studentship of G.I.

References

1 T. Tanaka, *Sci. Am.*, 1981, **244**, 124–138.
2 Q. Chai, Y. Jiao and X. Yu, *Gels*, 2017, **3**, 6.
3 G. Hild, *Prog. Polym. Sci.*, 1998, **23**, 1019–1149.
4 O. W. Webster, *Science*, 1991, **4996**, 887–893.
5 M. Vamvakaki, S. C. Hadjiyannakou, E. Loizidou, C. S. Patrickios, S. P. Armes and N. C. Billingham, *Chem. Mater.*, 2001, **13**, 4738–4744.
6 A. I. Triftaridou, D. Kafouris, M. Vamvakaki, T. K. Georgiou, T. C. Krasia, E. Themistou, N. Hadjiantoniou and C. S. Patrickios, *Polym. Bull.*, 2007, **58**, 185–190.
7 M. Vamvakaki, C. S. Patrickios, P. Lindner and M. Gradzielski, *Langmuir*, 2007, **23**, 10433–10437.
8 X. Zhang, K. Kyriakos, M. Rikkou-Kalourkoti, E. N. Kitiri, C. S. Patrickios and C. M. Papadakis, *Colloid Polym. Sci.*, 2016, **294**, 1027–1036.
9 M. Vamvakaki and C. S. Patrickios, *Chem. Mater.*, 2002, **14**, 1630–1638.
10 D. S. Achilleos, T. K. Georgiou and C. S. Patrickios, *Biomacromolecules*, 2006, **7**, 3396–3405.
11 S. N. Georgiades, M. Vamvakaki and C. S. Patrickios, *Macromolecules*, 2002, **35**, 4903–4911.
12 T. K. Georgiou and C. S. Patrickios, *Biomacromolecules*, 2008, **9**, 574–582.
13 E. Themistou and C. S. Patrickios, *Macromolecules*, 2004, **37**, 6734–6743.
14 D. Kafouris, E. Themistou and C. S. Patrickios, *Chem. Mater.*, 2006, **18**, 85–93.
15 E. Themistou and C. S. Patrickios, *Macromol. Chem. Phys.*, 2008, **209**, 1021–1028.
16 M. Rikkou-Kalourkoti, E. N. Kitiri, C. S. Patrickios, E. Leontidis, M. Constantinou, G. Constantinides, X. Zhang and C. M. Papadakis, *Macromolecules*, 2016, **49**, 1731–1742.
17 X. Zhang, K. Kyriakos, M. Rikkou-Kalourkoti, E. N. Kitiri, C. S. Patrickios and C. M. Papadakis, *Colloid Polym. Sci.*, 2016, **294**, 1027–1036.
18 E. N. Kitiri, C. S. Patrickios, C. Voutouri, T. Stylianopoulos, I. Hoffmann, R. Schweins and M. Gradzielski, *Polym. Chem.*, 2017, **8**, 245–259.
19 E. N. Kitiri, C. K. Varnava, C. S. Patrickios, C. Voutouri, T. Stylianopoulos, M. Gradzielski and I. Hoffmann, *J. Polym. Sci., Part A: Polym. Chem.*, 2018, **56**, 2161–2174.
20 N. Ghasdian, E. Church, A. P. Cottam, K. Hornsby, M. Y. Leung and T. K. Georgiou, *RSC Adv.*, 2013, **3**, 19070–19080.
21 O. W. Webster, W. R. Hertler, D. Y. Sogah, W. B. Farnham and T. V. RajanBabu, *J. Am. Chem. Soc.*, 1983, **105**, 5706–5708.
22 O. W. Webster, *Adv. Polym. Sci.*, 2004, **167**, 1–34.
23 T. K. Georgiou and C. S. Patrickios, *Macromolecules*, 2006, **39**, 1560–1568.
24 G. Moad, E. Rizzardo and S. H. Thang, *Aust. J. Chem.*, 2012, **65**, 985–1076.
25 J. Chiefari, Y. K. Chong, F. Ercole, J. Krstina, J. Jeffery, T. P. T. Le, R. T. A. Mayadunne, G. F. Meijs, C. L. Moad and G. Moad, *Macromolecules*, 1998, **31**, 5559–5562.
26 D. Prat, A. Wells, J. Hayler, H. Sneddon, C. R. McElroy, S. Abou-Shehada and P. J. Dunn, *Green Chem.*, 2016, **18**, 288–296.
27 N. Hadjichristidis, *J. Polym. Sci., Part A: Polym. Chem.*, 1999, **37**, 857–871.
28 J. M. Ren, T. G. McKenzie, Q. Fu, E. H. H. Wong, J. Xu, Z. An, S. Shanmugam, T. P. Davis, C. Boyer and G. G. Qiao, *Chem. Rev.*, 2016, **116**, 6743–6836.
29 H. Gao, M. C. Jones, J. Chen, R. E. Prud'homme and J. C. Leroux, *Chem. Mater.*, 2008, **20**, 3063–3067.
30 S. S. Nagarkar, M. Tsujimoto, S. Kitagawa, N. Hosono and S. Horike, *Chem. Mater.*, 2018, **30**, 8555–8561.
31 W. Xu, A. A. Steinschulte, F. A. Plamper, V. F. Korolovych and V. V. Tsukruk, *Chem. Mater.*, 2016, **28**(3), 975–985.
32 W. Wu, W. Wang and J. Li, *Prog. Polym. Sci.*, 2015, **46**, 55–85.
33 T. K. Georgiou, M. Vamvakaki, L. A. Phylactou and C. S. Patrickios, *Biomacromolecules*, 2005, **6**, 2990–2997.
34 T. K. Georgiou, L. A. Phylactou and C. S. Patrickios, *Biomacromolecules*, 2006, **7**, 3505–3512.
35 T. K. Georgiou, *Polym. Int.*, 2014, **63**, 1130–1133.
36 X. Liao, G. Walden, N. D. Falcon, S. Donell, M. J. Raxworthy, M. Wormstone, G. P. Riley and A. Saeed, *Eur. Polym. J.*, 2017, **87**, 458–467.
37 F. Dai, P. Sun, Y. Liu and W. Liu, *Biomaterials*, 2010, **31**, 559–569.
38 T. J. Gibson, P. Smyth, M. Semsarilar, A. P. McCann, W. J. McDaid, M. C. Johnston, C. J. Scott and E. Themistou, *Polym. Chem.*, 2020, **11**, 344–357.
39 K. S. Pafiti, C. S. Patrickios, T. K. Georgiou, E. N. Yamasaki, N. P. Mastroyiannopoulos and L. A. Phylactou, *Eur. Polym. J.*, 2012, **48**, 1422–1430.
40 M. Ahmed and R. Narain, *Prog. Polym. Sci.*, 2013, **38**, 767–790.
41 F. J. Xu, Z. X. Zhang, Y. Ping, J. Li, E. T. Kang and K. G. Neon, *Biomacromolecules*, 2009, **10**, 285–293.

42 T. K. Georgiou, M. Vamvakaki, C. S. Patrickios, E. N. Yamasaki and L. A. Phylactou, *Biomacromolecules*, 2004, **5**, 2221–2229.
43 D. P. Yang, M. N. N. L. Oo, G. R. Deen, Z. Li and X. J. Loh, *Macromol. Rapid Commun.*, 2017, **38**, 1700410.
44 J. Liu, H. Duong, M. R. Whittaker, T. P. Davis and C. Boyer, *Macromol. Rapid Commun.*, 2012, **33**, 760–766.
45 B. Jeong, Y. K. Choi, Y. H. Bae, G. Zentner and S. W. Kim, *J. Controlled Release*, 1999, **62**, 109–114.
46 J. Ferreira, J. Syrett, M. Whittaker, D. Haddleton, T. P. Davis and C. Boyer, *Polym. Chem.*, 2011, **2**, 1671–1677.
47 D. H. Rein, P. Rempp and P. J. Lutz, *Macromol. Chem. Phys.*, 1998, **199**, 569–574.
48 F. Dai, P. Sun, Y. Liu and W. Liu, *Biomaterials*, 2010, **31**, 559–569.
49 B. Mendrek, L. Sieroń, M. Libera, M. Smet, B. Trzebicka, A. L. Sieroń, A. Dworak and A. Kowalczuk, *Polymer*, 2014, **55**, 4551–4562.
50 Q. Qiu, G. Liu and Z. An, *Chem. Commun.*, 2011, **47**, 12685–12687.
51 X. Cao, C. Zhang, S. Wu and Z. An, *Polym. Chem.*, 2014, **5**, 4277–4284.
52 X. Shi, M. Miao and Z. An, *Polym. Chem.*, 2013, **4**, 1950–1959.
53 Q. Chen, X. Cao, H. Liu, W. Zhou, L. Qin and Z. An, *Polym. Chem.*, 2013, **4**, 4092–4102.
54 X. Shi, W. Zhou, Q. Qiu and Z. An, *Chem. Commun.*, 2012, **48**, 7389–7391.
55 K. Wang, H. Peng, K. J. Thurecht, S. Puttick and A. K. Whittaker, *Polym. Chem.*, 2014, **5**, 1760–1771.
56 B. S. Tucker, S. G. Getchell, M. R. Hill and B. S. Sumerlin, *Polym. Chem.*, 2015, **6**, 4258–4263.
57 Q. Chen, F. Han, C. Lin, X. Wen and P. Zhao, *Polymer*, 2018, **146**, 378–385.
58 J. F. Lutz, *J. Polym. Sci., Part A: Polym. Chem.*, 2008, **46**, 3459–3470.
59 E. Themistou and C. S. Patrickios, *Macromolecules*, 2007, **40**, 5231–5234.
60 K. Knop, R. Hoogenboom, D. Fischer and U. S. Schubert, *Angew. Chem., Int. Ed.*, 2010, **49**, 6288–6308.
61 V. Lotocki and A. Kakkar, *Pharmaceutics*, 2020, **12**, 827.
62 E. Themistou and C. S. Patrickios, *Macromolecules*, 2006, **39**, 73–80.
63 T. J. Gibson, P. Smyth, W. J. McDaid, D. Lavery, J. Thom, G. Cotton, C. J. Scott and E. Themistou, *ACS Macro Lett.*, 2018, **7**, 1010–1015.
64 P. Smyth, T. J. Gibson, G. Irvine, G. Black, D. Lavery, M. Semsarilar, C. J. Scott and E. Themistou, *Eur. Polym. J.*, 2020, **124**, 109471.
65 A. Blencowe, J. F. Tan, T. K. Goh and G. G. Qiao, *Polymer*, 2009, **50**, 5–32.
66 X. Wei, G. Moad, B. W. Muir, E. Rizzardo, J. Rosselgong, W. Yang and S. H. Thang, *Macromol. Rapid Commun.*, 2014, **35**, 840–845.
67 J. T. Wiltshire and G. G. Qiao, *Macromolecules*, 2006, **39**, 9018–9027.
68 P. Lang, W. Burchard, M. S. Wolfe, H. J. Spinelli and L. Page, *Macromolecules*, 1991, **24**, 1306–1314.
69 H. Gao and K. Matyjaszewski, *Macromolecules*, 2006, **39**, 7216–7223.
70 H. Gao, N. V. Tsarevsky and K. Matyjaszewski, *Macromolecules*, 2005, **38**, 5995–6004.
71 J. Hu, J. He, M. Zhang and P. Ni, *Polym. Chem.*, 2015, **6**, 1553–1566.
72 R. Banerjee, S. Parida, C. Maiti, M. Mandal and D. Dhara, *RSC Adv.*, 2015, **5**, 83565–83575.
73 M. Kawamura, A. Kanazawa, S. Kanaoka and S. Aoshima, *Polym. Chem.*, 2015, **6**, 4102–4108.
74 E. Themistou and C. S. Patrickios, *J. Polym. Sci., Part A: Polym. Chem.*, 2009, **47**, 5853–5870.
75 D. Delli Castelli, G. Ferrauto, J. C. Cutrin, E. Terreno and S. Aime, *Magn. Reson. Med.*, 2014, **71**, 326–332.
76 R. W. Ramette and E. B. Sandell, *J. Am. Chem. Soc.*, 1956, **78**, 4872–4878.
77 C. J. Miller, H. Yu and T. D. Waite, *Colloids Surf., A*, 2013, **435**, 147–153.
78 N. Pourreza, S. Rastegarzadeh and A. Larki, *Talanta*, 2008, **77**, 733–736.

